

Hydration of Gaseous Copper Dications Probed by IR Action Spectroscopy

Jeremy T. O'Brien and Evan R. Williams*

Department of Chemistry, University of California, Berkeley, California 94720-1460

Received: December 7, 2007; Revised Manuscript Received: April 4, 2008

Clusters of $\text{Cu}^{2+}(\text{H}_2\text{O})_n$, $n = 6\text{--}12$, formed by electrospray ionization, are investigated using infrared photodissociation spectroscopy, blackbody infrared radiative dissociation (BIRD), and density functional theory of select clusters. At 298 K, the BIRD rate constants increase with increasing cluster size for $n \geq 8$, but the trend reverses for the smaller clusters where $\text{Cu}^{2+}(\text{H}_2\text{O})_6$ is less stable than $\text{Cu}^{2+}(\text{H}_2\text{O})_8$. This trend in stability is consistent with a change in fragmentation pathway from loss of a water molecule for clusters with $n \geq 9$ to loss of hydrated protonated water clusters and the formation of the corresponding singly charged hydrated metal hydroxide for $n \leq 7$. The lowest-energy structures of $\text{Cu}^{2+}(\text{H}_2\text{O})_n$, $n = 6\text{--}8$ and 10, identified at the B3LYP/LACV3P**++ level of theory, all have coordination numbers (CN) of 4, although structures with a CN = 5 are within about 10 kJ/mol for all clusters except $\text{Cu}^{2+}(\text{H}_2\text{O})_8$. IR action spectra indicate the presence of hydrogen bonding for all clusters, and results for $\text{Cu}^{2+}(\text{H}_2\text{O})_n$, $n = 6\text{--}8$, are consistent with a CN = 4, although minor contributions from structures with higher CN cannot be ruled out. Bands in the action spectra of $\text{Cu}^{2+}(\text{H}_2\text{O})_n$, $n = 10\text{--}12$, show the presence of water molecules that accept two hydrogen bonds and donate one hydrogen bond as well as single hydrogen bond acceptors clearly indicating the onset for formation of a third solvent shell at a relatively small cluster size.

Introduction

Copper plays an important role in many biochemical processes, such as the activity of many enzymes,^{1–4} and is an essential element for human health. For example, abnormal regulation of cellular copper is connected to neurodegenerative diseases,^{3,4} including Alzheimer's disease.³ Redox properties of copper and copper complexes have been extensively studied, but some basic properties, such as the coordination number (CN) in water, are not unambiguously known. Cu^+ salts have low solubility in water ($K_{\text{sp}} < 10^{-7}$) which limits some solution-phase studies. By comparison, Cu^{2+} salts are readily dissolved in water and can be studied using a variety of methods. It is widely assumed that Cu^{2+} has a CN of 6, although coordination numbers ranging from 4 to 6 have been indicated from results of X-ray absorption spectroscopy,^{2,5–7} neutron diffraction,^{8,9} infrared spectroscopy,⁷ and computational studies.^{9–13} Hydration of Cu^{2+} is especially interesting because the d^9 electronic configuration results in Jahn–Teller distortion characterized by two elongated axial bonds in octahedral structures. Ambiguity about the structure of the first solvation shell has been attributed in part to structural assumptions in the fitting procedures necessary to analyze X-ray absorption spectra and the inability to distinguish axial Cu–O from overlapping Cu–H correlations in neutron diffraction studies.⁹ There may be no clearly preferred structure but rather rapidly interconverting structures that have coordination numbers ranging from 4 to 6.⁵

Insights into the hydration of ions in solution can potentially be obtained by investigating hydrated clusters in the gas phase.^{14–39} Structures can be examined as a function of cluster size to reveal evidence for shell formation or other uniquely stable structures, such as clathrates for some protonated and other ion-containing water clusters.^{18,19} Electrospray ionization (ESI) has made possible the production of hydrated metal

dications and even trications⁴⁰ for a wide variety of metal ions. $\text{Cu}^{2+}(\text{H}_2\text{O})_n$ was first produced by ESI,⁴¹ but these clusters can also be produced using a pickup technique in which water molecules are condensed onto neutral copper atoms and subsequently are ionized by electron impact.^{33,42} The dissociation of hydrated divalent ions has been extensively investigated.^{24–33,42–44} In general, activation of hydrated divalent ions results in sequential loss of water molecules for larger clusters, but a charge-separation reaction typically occurs for small clusters in which H_3O^+ and the corresponding hydrated metal hydroxide with a single charge is produced. The cluster size at which the transition between these two reaction pathways is observed depends on ion identity as well as on activation conditions.³⁰ A salt-bridge mechanism in which proton transfer occurs from the first solvation shell to a water molecule in the second shell has been proposed for the charge-separation reaction,⁴³ and both experimental and computational data supporting this mechanism for several hydrated ions have been reported.^{36–39}

Duncombe et al. investigated the formation and dissociation of $\text{Cu}^{2+}(\text{H}_2\text{O})_n$ and $\text{Cu}^{2+}(\text{NH}_3)_n$ and found that these clusters with eight ligands are the most abundant in the mass spectrum.³³ For $\text{Cu}^{2+}(\text{H}_2\text{O})_n$, water loss occurs for clusters with $n \geq 7$ whereas charge separation occurs for $n = 6\text{--}8$.^{30,33,44} In contrast to results for some other hydrated divalent metal ions,^{36–38,43} both mono- and dihydrated H_3O^+ is produced in the charge-separation reaction. A salt-bridge mechanism analogous to that of Beyer et al.,⁴³ but in which a second water molecule coordinates to the H_3O^+ before charge separation occurs, has been proposed.³⁹ On the basis of their results for gas-phase clusters, Duncombe et al. concluded that $\text{Cu}^{2+}(\text{H}_2\text{O})_8$ was of special significance and that the structure of this ion may play an important role in aqueous solution.³³ Density functional theory (DFT) calculations reported by Bérces et al. on clusters with $n = 3\text{--}8$ indicate that the CN of $\text{Cu}^{2+}(\text{H}_2\text{O})_n$ is 4 and that the first solvation shell for clusters containing up to eight water molecules is square planar.⁴⁵ The stability of $\text{Cu}^{2+}(\text{H}_2\text{O})_8$ was

* To whom correspondence should be addressed. Fax: (510) 642-7714; e-mail: Williams@cchem.berkeley.edu.

attributed to each of the four water molecules in the second shell accepting two hydrogen bonds from the four water molecules in the inner shell, and it was concluded that the gas-phase shell development does not properly reflect that in solution when a limited number of solvent molecules are considered.⁴⁵

Information about ion–water interactions and coordination numbers can be obtained from infrared (IR) action spectroscopy of hydrated ions,^{16–23,46–49} although this method has only recently been applied to investigating shell structures of hydrated metal dications.²⁰ The frequencies of OH stretching vibrations can shift substantially with changes in the hydrogen bonding of the water molecule making this method especially well suited for structural elucidation of hydrated ions. For example, the IR action spectrum of $\text{Cu}^+(\text{H}_2\text{O})_3\text{Ar}$ has a bonded OH feature that is clearly observed at 2980 cm^{-1} , a $> 600\text{ cm}^{-1}$ shift from the free-OH stretching region of $3600\text{--}3700\text{ cm}^{-1}$, indicating that even with only three water molecules, one of the water molecules coordinating to the metal ion donates a hydrogen bond to a second-shell water molecule.⁴⁸

Here, structures of $\text{Cu}^{2+}(\text{H}_2\text{O})_n$, $n = 6\text{--}12$, are probed using IR action spectroscopy, blackbody infrared radiative dissociation (BIRD), and hybrid density functional theory. From these studies, new insights into the hydration of copper dication and its shell structures are obtained.

Experimental Section

Mass Spectrometry. All experiments were performed on a 2.75 T Fourier transform ion cyclotron resonance mass spectrometer.^{20,40,50} Distributions of $\text{Cu}^{2+}(\text{H}_2\text{O})_n$ were produced by nanoelectrospray ionization of a 4 mM aqueous solution of CuSO_4 (Fischer Scientific, Waltham, MA). These clusters were introduced into the mass spectrometer and were trapped in a cylindrical ion cell that is surrounded by a copper jacket cooled to 215 K by a regulated flow of liquid nitrogen.²⁷ The copper jacket temperature was allowed to equilibrate for at least 8 h prior to the experiments. Ions were accumulated in the cell for 4–6 s during which time dry N_2 gas ($\sim 10^{-6}$ Torr) was pulsed into the vacuum chamber using a piezoelectric valve to enhance trapping and thermalization of the ions. A mechanical shutter was subsequently closed to prevent further ion accumulation, and residual gases were pumped out for 6–10 s resulting in a base pressure of $\sim 10^{-8}$ Torr prior to ion isolation.

$\text{Cu}^{2+}(\text{H}_2\text{O})_7$ was the smallest cluster observed directly by ESI under a wide range of source conditions. $\text{Cu}^{2+}(\text{H}_2\text{O})_6$ was formed by collisionally activating larger clusters using a frequency sweep or chirp excitation waveform ($200\text{ }\mu\text{s}$, $2000\text{ Hz}/\mu\text{s}$, $\sim 250\text{ V}_{\text{pk-pk}}$) that increased the average velocity of all trapped ions with $m/z > 90$. This excitation was repeated nine times with a 300 ms delay between each chirp to maximize the intensity of $\text{Cu}^{2+}(\text{H}_2\text{O})_6$. Dry N_2 was pulsed into the chamber ($\sim 10^{-6}$ Torr) during this time to enhance collisional activation, and residual gases were then pumped out for 10 s prior to isolation of this ion.

The cluster of interest was isolated using a stored waveform inverse Fourier transform. To obtain IR action spectra, the isolated clusters were irradiated using tunable IR light produced by an optical parametric oscillator/amplifier (OPO/OPA) system (LaserVision, Bellevue, WA) pumped by the fundamental of a Nd:YAG laser (Continuum Surelight I-10, Santa Clara, CA) at a 10 Hz repetition rate. Laser irradiation times were varied from 1 to 20 s to improve the dynamic range and the signal-to-noise of the IR spectrum. Typically, 1 or 3 s irradiation times were used for frequencies in the free-OH stretch region ($3600\text{--}3750\text{ cm}^{-1}$) of the IR spectrum; otherwise, a 20 s irradiation time

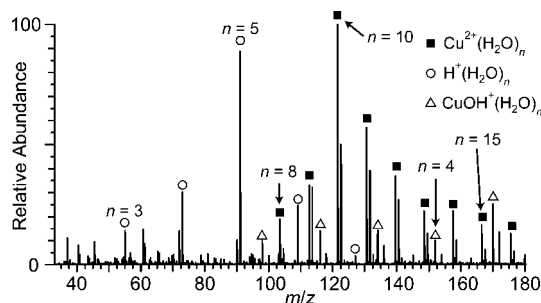


Figure 1. A representative electrospray ionization mass spectrum of a 4 mM aqueous CuSO_4 solution with the copper jacket that surrounds the ion cell at 215 K. Distributions of $\text{Cu}^{2+}(\text{H}_2\text{O})_n$, $\text{CuOH}^+(\text{H}_2\text{O})_n$, and $\text{H}_3\text{O}^+(\text{H}_2\text{O})_n$ are indicated on the spectrum.

was used. From the abundances of the precursor and product ions, dissociation rates as a function of the IR laser frequency were obtained. These dissociation rates were corrected for the BIRD background dissociation, the differences in laser power at different frequencies, and the duration of laser irradiation. To obtain unimolecular dissociation rate constants for both laser photodissociation at a specific frequency and for BIRD,^{24–27} ions were exposed to radiation for up to 50 s, and these data were fit to first-order kinetics. All data were acquired using a MIDAS⁵¹ modular data system.

Computational Chemistry. Candidate low-energy structures were identified using conformational searching and previously reported low-energy structures.⁴⁵ Initial structures were generated using 10 000 step Monte Carlo conformational searching as implemented in MacroModel 8.1 (Schrödinger, Inc., Portland, OR) using the MMFF94 force field. The conformation searching generated primarily structures with $\text{CN} = 6$. To obtain structures with $\text{CN} = 4$ and 5 similar to those reported previously,⁴⁵ water molecules were manually rearranged from structures with $\text{CN} = 6$.

These candidate structures were geometry optimized, and the self-consistent field (SCF) energy was calculated with B3LYP hybrid density functional calculations using the LACV3P**++ basis set as implemented in Jaguar v. 6.5 (Schrödinger, Inc., Portland, OR). Harmonic vibrational frequencies and intensities were calculated using the numerical derivatives of the LACV3P**++ energy-minimized Hessian. All structures yielded positive frequency modes indicating that they are local-minimum structures. The energies reported are the relative Gibbs free energies at 215 K, the temperature of the copper jacket in the experimental measurements, and include zero-point energy corrections. Relative electronic energies are reported for comparison to previous results for $\text{Cu}^{2+}(\text{H}_2\text{O})_6$. Structures were energy-minimized, and vibrational frequencies and intensities were calculated for the low-energy structures of $\text{Cu}^{2+}(\text{H}_2\text{O})_6$ at the BP86/LACV3P**++ level of theory. All vibrational frequencies are scaled by 0.956 which has been shown previously to provide good agreement with experimental IR spectra in the free-OH region.²² To approximate temperature and other broadening effects, the calculated line spectra are convolved using 15 and 50 cm^{-1} full width at half-maximum (fwhm) Lorentzian distributions for the nonbonded and bonded features, respectively.

Results and Discussion

Ion Formation. Electrospray ionization of a 4 mM solution of aqueous CuSO_4 results in broad distributions of $\text{Cu}^{2+}(\text{H}_2\text{O})_n$, $\text{CuOH}^+(\text{H}_2\text{O})_n$, and $\text{H}^+(\text{H}_2\text{O})_n$. A typical ESI spectrum is shown in Figure 1. The size and width of these distributions depend on ion source and other instrumental parameters and can

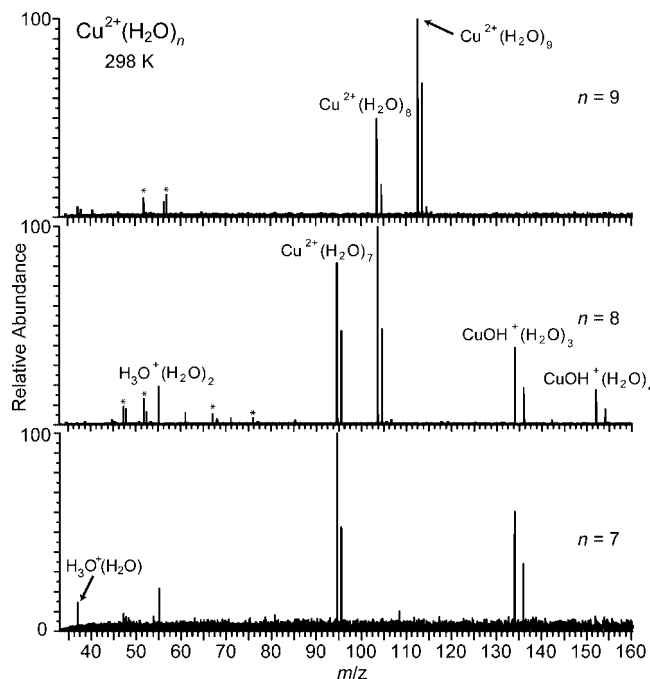
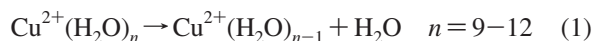


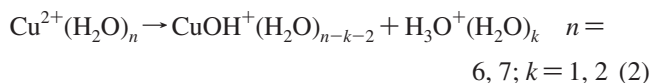
Figure 2. BIRD spectra of isolated $\text{Cu}^{2+}(\text{H}_2\text{O})_n$, $n = 7-9$, measured with a copper jacket temperature of 298 K and 20, 25, and 0.5 s reaction times for $n = 7, 8$, and 9 , respectively. Harmonics of the fundamental frequencies of trapped ions are marked with an “*”.

generally be shifted to the cluster size of interest by adjusting these parameters.⁴⁰ Although $\text{Cu}^{2+}(\text{H}_2\text{O})_8$ can be made the base peak in the spectrum, its abundance does not stand out from that of its neighboring clusters under a wide range of conditions (Figure 1). $\text{Cu}^{2+}(\text{H}_2\text{O})_7$ is the smallest dication copper cluster observed consistent with earlier results of hydrated dication copper ions formed by ESI.⁴¹ Clusters as small as $\text{Cu}^{2+}(\text{H}_2\text{O})_2$ were observed by Duncombe et al. with the pickup technique,³³ and clusters with n between 1 and 6 have been produced by collisional activation of $\text{Cu}^{2+}(\text{H}_2\text{O})_{n>6}$.^{30,33,44} To form $\text{Cu}^{2+}(\text{H}_2\text{O})_6$ in this experiment, the broad distribution of ions trapped in the Fourier transform ion cyclotron resonance (FT/ICR) cell are collisionally activated using a series of frequency sweep or chirp excitation pulses. No smaller hydrated Cu^{2+} clusters were observed over a wide range of conditions.

Ion Fragmentation and Stability. BIRD spectra of isolated $\text{Cu}^{2+}(\text{H}_2\text{O})_n$, $n = 7-9$, measured at a cell temperature of 298 K and at 20, 25, and 0.5 s reaction times for $n = 7, 8$, and 9 , respectively, are shown in Figure 2. BIRD of isolated $\text{Cu}^{2+}(\text{H}_2\text{O})_n$, $n = 9-12$, results in consecutive loss of a neutral water molecules.



For $n = 6$ and 7 , a charge-separation reaction takes place resulting in formation of protonated water clusters and the corresponding hydrated $(\text{CuOH})^+$.



For $\text{Cu}^{2+}(\text{H}_2\text{O})_8$, fragment ions from both reactions are formed in roughly equal proportions (Figure 2). These results are consistent with the metastable fragmentation pathways reported by Duncombe et al., although in that study, some neutral water loss from $\text{Cu}^{2+}(\text{H}_2\text{O})_7$ was also observed.³³ By comparison, $\text{Cu}^{2+}(\text{H}_2\text{O})_n$, $n = 1-6$, can be produced by collisional activation

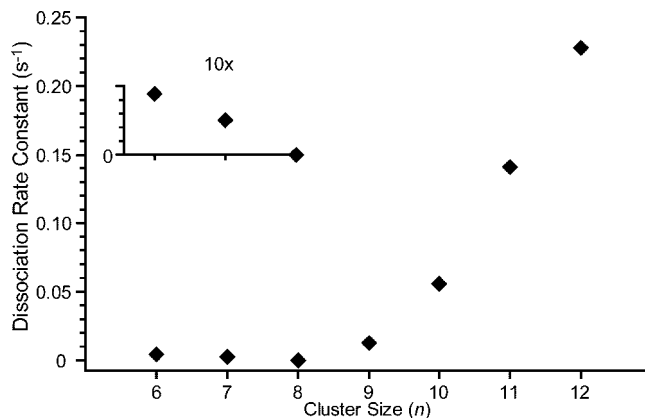


Figure 3. BIRD rate constants of $\text{Cu}^{2+}(\text{H}_2\text{O})_n$, $n = 6-12$, with a copper jacket temperature of 215 K.

of $\text{Cu}^{2+}(\text{H}_2\text{O})_{n>6}$.^{30,33,44} With the relatively long time scale of these BIRD experiments, low-energy dissociation processes are favored compared to activating ions by energetic collisions. Thus, formation of $\text{CuOH}(\text{H}_2\text{O})_n^+$ under the lower-energy activation conditions of BIRD used here indicates that loss of a water molecule is entropically favored over the charge-separation reaction consistent with previous results for $\text{SO}_4^{2-}(\text{H}_2\text{O})_n$.⁵²

Dissociation rate constants in the zero-pressure limit⁵³⁻⁵⁵ were obtained from BIRD spectra as a function of reaction times up to 50 s at 215 K. The temperature of 215 K was chosen so that the lifetimes of $\text{Cu}^{2+}(\text{H}_2\text{O})_{10-12}$ are sufficiently long that IR action spectra can be readily measured. These rate constants as a function of cluster size are shown in Figure 3. For $n \geq 8$, the BIRD rate constant increases with cluster size. This can be attributed both to a decrease in water-binding energy²⁴⁻²⁹ and to an increase in the rate of absorption of blackbody radiation⁵⁴ with increasing cluster size. Surprisingly, the trend in ion stability reverses at $n = 8$, where the $n = 7$ and $n = 6$ clusters are progressively less stable. This can be attributed to a lower barrier for the charge-separation reaction versus water loss as well as to possible ion structure effects. The higher stability of the $n = 7$ compared to $n = 6$ cluster indicates that the barrier for the charge-separation reaction decreases with cluster size over this range.

The stabilities of these clusters alone do not provide significant insights into structures. Additional studies aimed at determining water-binding energies or entropies may provide more useful insights into shell structures.

IR Action Spectroscopy and Free-OH Stretches. Infrared action spectra from ~ 2800 to 3800 cm^{-1} for $\text{Cu}^{2+}(\text{H}_2\text{O})_{6-12}$ measured with the ion cell temperature at 215 K are shown in Figure 4. The spectra for $\text{Cu}^{2+}(\text{H}_2\text{O})_{6-9}$ each have two bands in the high-frequency region at $\sim 3600 \text{ cm}^{-1}$ and $\sim 3660 \text{ cm}^{-1}$ consistent with the respective symmetric (ν_{sym}) and asymmetric (ν_{asym}) free-OH stretch frequencies of water molecules that do not donate any hydrogen bonds (acceptor-only molecules). Dangling-OH stretch frequencies from water molecules that donate a single hydrogen bond can also contribute to the band at $\sim 3660 \text{ cm}^{-1}$. These bands can be readily identified as free-OH stretches on the basis of comparison to previously reported IR action spectra of hydrated metal ion clusters, such as $\text{Ca}^{2+}(\text{H}_2\text{O})_{4-9}$,²⁰ $\text{Ni}^+(\text{H}_2\text{O})_{1-5}$,²¹ $\text{Cs}^+(\text{H}_2\text{O})_{1-5}$,²³ and $\text{H}_3\text{O}^+(\text{H}_2\text{O})_{3-8}$.¹⁵⁻¹⁷ The frequencies of these vibrations are substantially red-shifted from those of an isolated water molecule (3649 cm^{-1} and 3731 cm^{-1} , respectively)⁵⁶ or free-OH stretches of $\text{Ni}^+(\text{H}_2\text{O}) \cdot \text{Ar}_2$ (3623 cm^{-1} and 3696 cm^{-1})²¹ because of partial electron transfer

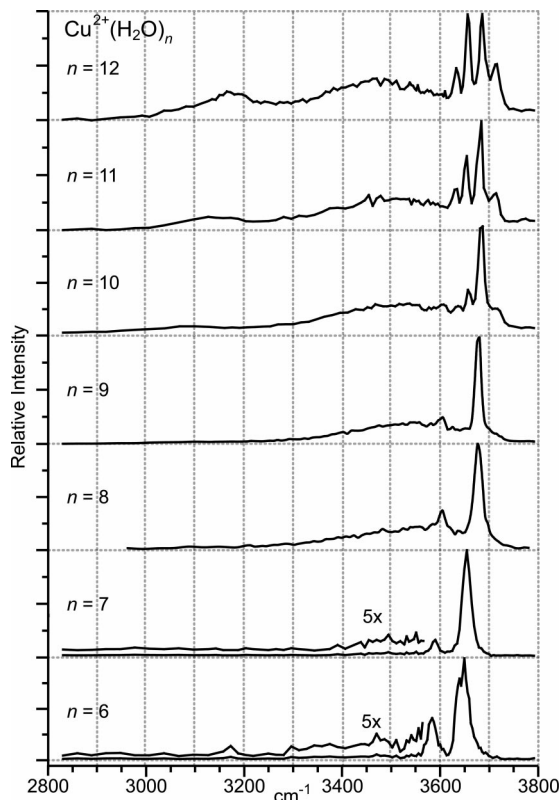


Figure 4. Infrared action spectra of $\text{Cu}^{2+}(\text{H}_2\text{O})_n$, $n = 6-12$, obtained with a copper jacket temperature of 215 K. The cluster size (n) is indicated for each spectrum.

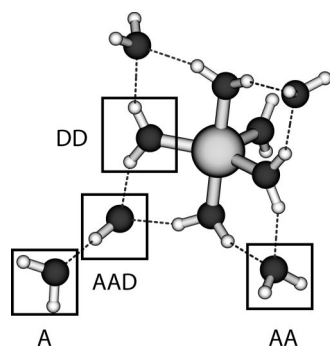


Figure 5. Hydrogen bonding motifs: A = single acceptor, AA = double acceptor, DD = double donor, AAD = acceptor-acceptor-donor.

from the water molecules to the cation which leads to weaker O–H bonding and lower frequency vibrations.²¹ These peaks for $\text{Cu}^{2+}(\text{H}_2\text{O})_{6-12}$ blue shift with increasing cluster size because the magnitude of the electron transfer per water molecule decreases. Similar trends have been observed in the spectra of both $\text{H}_3\text{O}^+(\text{H}_2\text{O})_n$ ^{17,18} and $\text{Ca}^{2+}(\text{H}_2\text{O})_n$.²⁰

In contrast, spectra of $\text{Cu}^{2+}(\text{H}_2\text{O})_{10-12}$ have four distinct features in this region which become more pronounced with increasing cluster size. All of these features are characteristic of different free-OH stretching vibrations in hydrated clusters, and these hydrogen bonding motifs are illustrated in Figure 5.¹⁵⁻²⁰ These bands can be assigned on the basis of previously reported IR action spectra of $\text{H}_3\text{O}^+(\text{H}_2\text{O})_{7-20}$ ¹⁵⁻¹⁹ and the calculated spectra of low-energy structures (vide infra). The peaks at $\sim 3640\text{ cm}^{-1}$ and $\sim 3725\text{ cm}^{-1}$ are consistent with the free-OH ν_{sym} and ν_{asym} , respectively, of water molecules that accept a single hydrogen bond, that is, single acceptor (A) molecules. The band at $\sim 3660\text{ cm}^{-1}$ is due to the ν_{asym} of water

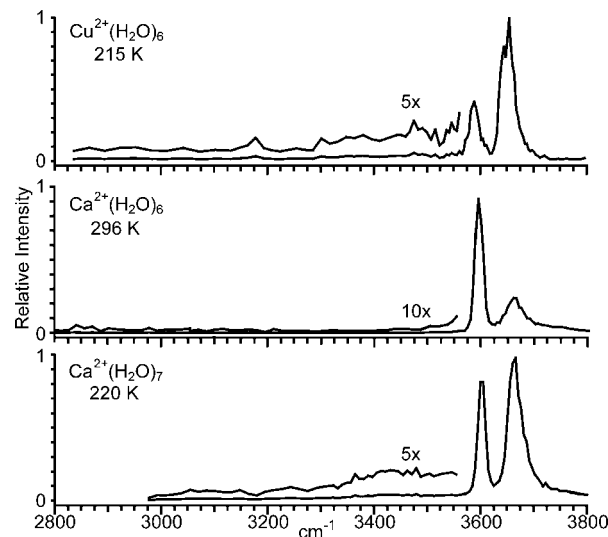


Figure 6. Infrared action spectra of $\text{Cu}^{2+}(\text{H}_2\text{O})_6$, $\text{Ca}^{2+}(\text{H}_2\text{O})_6$, and $\text{Ca}^{2+}(\text{H}_2\text{O})_7$ measured at the indicated temperature. The hydrated divalent calcium spectra are replotted from ref 20.

molecules that accept two hydrogen bonds and donate one, that is, acceptor-acceptor-donors (AAD). The band at $\sim 3690\text{ cm}^{-1}$ is the ν_{asym} of water molecules that accept two hydrogen bonds (AA) blue-shifted from the corresponding vibration in the smaller clusters.

Hydrogen-Bonded OH Stretches. Two bands corresponding to hydrogen-bonded stretches are identified in the $\text{Cu}^{2+}(\text{H}_2\text{O})_n$ IR action spectra: a very broad band from ~ 3300 to 3600 cm^{-1} that is clearly present for $n = 8-12$ and a second broad feature ($\sim 3000-3300\text{ cm}^{-1}$) in the spectra of $\text{Cu}^{2+}(\text{H}_2\text{O})_{10-12}$. Weak photodissociation occurs for $\text{Cu}^{2+}(\text{H}_2\text{O})_{6,7}$ in the region between ~ 3200 and 3500 cm^{-1} . Similarly broad OH bonded features have been observed in the IR spectra of $\text{Cu}^+(\text{H}_2\text{O})_n$,⁴⁸ $\text{Ni}^+(\text{H}_2\text{O})_n$,²¹ $\text{Ca}^{2+}(\text{H}_2\text{O})_n$,²⁰ and $\text{H}_3\text{O}^+(\text{H}_2\text{O})_n$.¹⁶⁻¹⁹ On the basis of earlier studies, the very broad feature centered near 3500 cm^{-1} for the larger clusters is assigned to the hydrogen-bonded OH stretches of double-donor (DD) water molecules. The photodissociation between 3300 and 3500 cm^{-1} for $\text{Cu}^{2+}(\text{H}_2\text{O})_{6,7}$ is consistent with DD water molecules indicating that some population of the clusters contain at least two water molecules in the second solvation shell. The band centered around 3100 cm^{-1} in the larger clusters coincides with the appearance of the AAD ν_{asym} free-OH peak and is consistent with results from protonated water clusters for which a band in the same region is assigned to the hydrogen-bonded ν_{sym} OH stretches of AAD water molecules.¹⁸

Comparison to Divalent Calcium. Some useful insights into the structures of $\text{Cu}^{2+}(\text{H}_2\text{O})_n$ can be obtained by comparing data for hydrated divalent calcium, which has a larger ionic radii (1.00 \AA , CN = 6) compared to that for copper (0.73 \AA , CN = 6).⁵⁷ IR action spectra of $\text{Cu}^{2+}(\text{H}_2\text{O})_6$ and $\text{Ca}^{2+}(\text{H}_2\text{O})_{6,7}$ are shown in Figure 6. The relative intensities of the ν_{sym} and ν_{asym} free-OH stretches of $\text{Cu}^{2+}(\text{H}_2\text{O})_6$ more closely resembles that of $\text{Ca}^{2+}(\text{H}_2\text{O})_7$ than that of $\text{Ca}^{2+}(\text{H}_2\text{O})_6$. $\text{Ca}^{2+}(\text{H}_2\text{O})_6$ has an octahedral structure (CN = 6) on the basis of BIRD,²⁴⁻²⁶ guided ion beam,²⁹ spectroscopic,²⁰ and computational^{20,29} results. Some of these studies indicate that $\text{Ca}^{2+}(\text{H}_2\text{O})_7$ also has a CN = 6 although a heptacoordinated structure is not ruled out.²⁵ Spectroscopic evidence indicates the presence of at least two different structures of this ion in which an outer shell water molecule accepts either one (A) or two (AA) hydrogen bonds from inner-shell water molecules.²⁰

The free-OH stretches in the $\text{Cu}^{2+}(\text{H}_2\text{O})_6$ spectrum are red-shifted by $\sim 10\text{ cm}^{-1}$ compared to the corresponding bands in the $\text{Ca}^{2+}(\text{H}_2\text{O})_6$ spectrum. This indicates greater electron transfer from the water molecules to the Cu^{2+} consistent with the smaller size and therefore greater charge density of Cu^{2+} . The intensity of the ν_{sym} band relative to that of the ν_{asym} band for $\text{Cu}^{2+}(\text{H}_2\text{O})_6$ is substantially smaller than that for $\text{Ca}^{2+}(\text{H}_2\text{O})_6$ and is much closer to that of $\text{Ca}^{2+}(\text{H}_2\text{O})_7$. The significantly lower intensity of ν_{sym} compared to ν_{asym} has been observed in many other action spectra of large hydrated clusters.^{18–21,48} The relative intensities of these bands are related to the structure of the cluster and to the extent of hydrogen bonding^{17–21,34} and for $\text{Ca}^{2+}(\text{H}_2\text{O})_n$ ²⁰ and $\text{Ni}^{2+}(\text{H}_2\text{O})_n$ ²¹ are indicative of the onset for second-shell formation. This ratio for the $\text{Cu}^{2+}(\text{H}_2\text{O})_6$ also suggests that one or more water molecules are in the second shell, although structural differences between $\text{Cu}^{2+}(\text{H}_2\text{O})_n$ and $\text{Ca}^{2+}(\text{H}_2\text{O})_n$ will almost certainly affect this ratio as well.

A region of the spectrum that is potentially more indicative of water molecules in a second shell is the lower frequency region between 3000 and 3500 cm^{-1} , which corresponds to the OH stretching region of inner-shell water molecules involved in hydrogen bonding to outer-shell water molecules. Some photodissociation in this region is observed for $\text{Cu}^{2+}(\text{H}_2\text{O})_6$, although the intensity is very low. By comparison, significantly more photodissociation in this region is observed for $\text{Ca}^{2+}(\text{H}_2\text{O})_7$ than for $\text{Ca}^{2+}(\text{H}_2\text{O})_6$, although the photodissociation intensity in this region for $\text{Ca}^{2+}(\text{H}_2\text{O})_7$ is much less than that expected on the basis of calculated absorption spectra for structures containing a second-shell water molecule.²⁰

The laser photodissociation rate at 3450 cm^{-1} for $\text{Cu}^{2+}(\text{H}_2\text{O})_6$ is only about 2 times higher than the BIRD rate. To ascertain if this laser-induced photodissociation is significant and indicates the presence of a second-shell water molecule or molecules, data were acquired as a function of time for reaction times up to 50 s. The data for $\text{Cu}^{2+}(\text{H}_2\text{O})_6$ were acquired at 215 K, the temperature at which the spectra were obtained. The data for $\text{Ca}^{2+}(\text{H}_2\text{O})_6$ were acquired at both 296 (data not shown) and 335 K (Figure 7). The latter temperature was chosen so that the BIRD rate would be comparable to that for $\text{Cu}^{2+}(\text{H}_2\text{O})_6$ at 215 K. Measurement of laser photodissociation kinetics under conditions where the BIRD rates of the two ions are comparable should compensate for the different dissociation energies of these two ions so that absorption of one or more laser generated photons should produce comparable dissociation despite the different dissociation energies. These data are fit to first-order kinetics, and the rate constants are reported in Table 1.

Laser photodissociation data, obtained under the same conditions as the BIRD data and at 3450 and 3655 cm^{-1} for $\text{Cu}^{2+}(\text{H}_2\text{O})_6$ and at 3450 and 3610 cm^{-1} for $\text{Ca}^{2+}(\text{H}_2\text{O})_6$, are shown in Figure 7. The two higher frequencies are where maximum photodissociation occurs in the IR action spectrum of each cluster. The lower frequency corresponds to an approximate maximum in the hydrogen-bonding band in the $\text{Cu}^{2+}(\text{H}_2\text{O})_8$ spectrum, the smallest cluster in which a distinct hydrogen-bonding feature is clearly observed. These data fit first-order kinetics, and laser-induced photodissociation rate constants are obtained from the difference of the total dissociation and BIRD rate constants. These values are given in Table 1.

From the ratio of the laser-induced photodissociation rate constants at the two photon energies, a comparison of the relative extent of fragmentation that occurs in the hydrogen-bonding region of the spectrum of $\text{Cu}^{2+}(\text{H}_2\text{O})_6$ to that of $\text{Ca}^{2+}(\text{H}_2\text{O})_6$ is obtained (Table 1). For $\text{Ca}^{2+}(\text{H}_2\text{O})_6$, the laser-induced photodissociation rate constant at 3450 cm^{-1} is ~ 450 times smaller

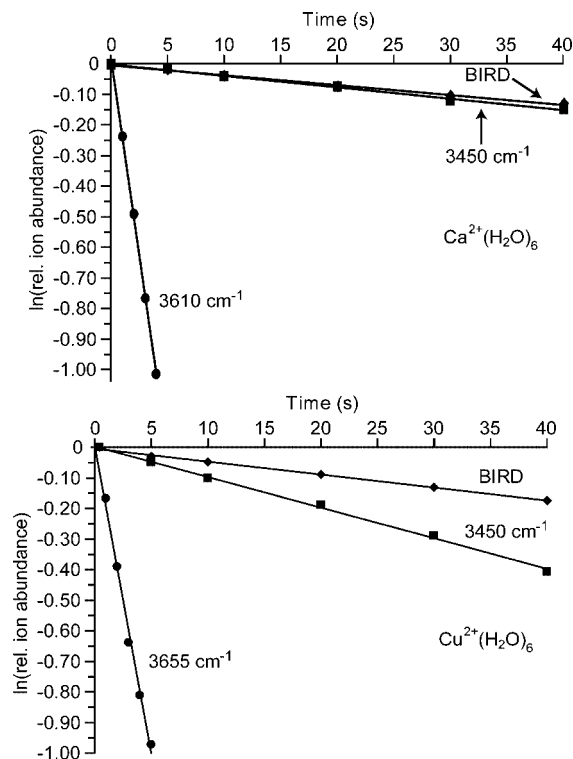


Figure 7. BIRD and laser photodissociation data at the frequencies indicated in the plots for $\text{Cu}^{2+}(\text{H}_2\text{O})_6$ and $\text{Ca}^{2+}(\text{H}_2\text{O})_6$ with a copper jacket temperature of 215 and 335 K, respectively.

than that at 3610 cm^{-1} . In sharp contrast, this rate constant for $\text{Cu}^{2+}(\text{H}_2\text{O})_6$ at 3450 cm^{-1} is 60 times smaller than that where maximum dissociation occurs. Thus, there is ~ 8 times more relative dissociation in the hydrogen-bonding region for $\text{Cu}^{2+}(\text{H}_2\text{O})_6$ compared to that for $\text{Ca}^{2+}(\text{H}_2\text{O})_6$. These data indicate the presence of hydrogen bonding for the $\text{Cu}^{2+}(\text{H}_2\text{O})_6$ cluster and illustrate the advantage of the high signal-to-noise ratio that is possible in these experiments for identifying weak, but structurally significant, features.

For the $\text{Ca}^{2+}(\text{H}_2\text{O})_6$ data at 295 K, the laser-induced photodissociation rate constant at 3450 cm^{-1} is almost 1000 times smaller than that at 3610 cm^{-1} . The lower dissociation efficiency at the lower temperature and frequency suggests that some of the photodissociation can be attributed to absorption of more than one photon under these conditions. By increasing the temperature, a greater fraction of the population can be dissociated upon absorption of a single photon.

Computations. More detailed structural information can be obtained by comparing the experimentally measured IR action spectra to calculated absorption spectra of candidate low-energy structures. The relative electronic energies as well as Gibbs free energies at the temperature of the spectroscopy experiments (215 K) are reported in Table 2 for $\text{Cu}^{2+}(\text{H}_2\text{O})_n$, $n = 6–8, 10$. The lowest-energy structure for each cluster size is found to be very similar to those identified by Bérces et al. who used the BP86 density functional and Slater function basis sets.⁴⁵ The only minor structural differences are the orientations of some water molecules; tetrahedral bonding of water molecules is favored by the BP86 functional whereas more planar bonding is favored by B3LYP.⁴⁵ However, the energy differences between different structures are substantially smaller at the B3LYP/LACV3P**++ level of theory. Relative electronic energies from calculations for $\text{Cu}^{2+}(\text{H}_2\text{O})_6$ at the BP86/LACV3P**++ level of theory are compared to those reported by Bérces et al.⁴⁵ (Table 2). These values are within 10 kJ/mol of the previously reported values,⁴⁵

TABLE 1: Dissociation Rate Constants (s^{-1}) for $\text{Cu}^{2+}(\text{H}_2\text{O})_6$ and $\text{Ca}^{2+}(\text{H}_2\text{O})_6^a$

	k_{max} (s^{-1})	k_{3450} (s^{-1})	k_{BIRD} (s^{-1})	BIRD corrected k_{max}/k_{3450}
$\text{Cu}^{2+}(\text{H}_2\text{O})_6$	0.22 ± 0.01	$8.1 \times 10^{-3} \pm 4 \times 10^{-4}$	$4.6 \times 10^{-3} \pm 2 \times 10^{-4}$	61
$\text{Ca}^{2+}(\text{H}_2\text{O})_6$ (296 K)	0.15 ± 0.008	$1.6 \times 10^{-4} \pm 8 \times 10^{-6}$	$4.0 \times 10^{-5} \pm 5 \times 10^{-6}$	954
$\text{Ca}^{2+}(\text{H}_2\text{O})_6$ (335 K)	0.26 ± 0.004	$3.8 \times 10^{-3} \pm 1 \times 10^{-4}$	$3.2 \times 10^{-3} \pm 1 \times 10^{-4}$	433

^a At copper jacket temperatures of 215 K for $\text{Cu}^{2+}(\text{H}_2\text{O})_6$ and at both 296 and 335 K for $\text{Ca}^{2+}(\text{H}_2\text{O})_6$. Obtained from the slopes of Figure 7 data; the laser frequency of k_{max} is 3655 cm^{-1} and 3610 cm^{-1} for $\text{Cu}^{2+}(\text{H}_2\text{O})_6$ and $\text{Ca}^{2+}(\text{H}_2\text{O})_6$, respectively.

TABLE 2: Relative Gibbs free energies (kJ/mol) at 215 K and Relative Electronic Energies for Select Structures of $\text{Cu}^{2+}(\text{H}_2\text{O})_n$, $n = 6-8$ and 10^a

structure	B3LYP		BP86	
	LACV3P**++	relative electronic energies	LACV3P**++	Slater
	relative Gibbs free energies		relative electronic energies	previous work ^b
6AI	0	1	0	0
6AII	3	0	3	13
6B	9	13	22	29
6C	22	37	61	71
7A	0	0		
7B	11	15		
7C	38	46		
8A	0	0		
8B	21	21		
8C	40	53		
10A	0	0		
10B	10	5		
10C	32	31		

^a From B3LYP/LACV3P**++ calculations and relative electronic energies from BP86 calculations. ^b From ref 45.

but the energy differences between structures with B3LYP/LACV3P**++ are substantially lower. This indicates that although the ordering of the stabilities of the different structures is nearly the same, the magnitude of the energetic differences depends strongly on the density functional used.

For all these clusters, structures with a CN = 4 were found to be most stable. For all but $\text{Cu}^{2+}(\text{H}_2\text{O})_8$, structures with a CN = 5 are $\sim 10 \text{ kJ/mol}$ less stable at 215 K. Structures with CN = 6 are more than 20 kJ/mol less stable. As noted previously for $\text{Cu}^{2+}(\text{H}_2\text{O})_8$,^{33,45} there is a clear preference for a CN = 4 structure because of an especially favorable hydrogen bond network.

Comparisons to Experimental Data. Vibrational frequencies and intensities were calculated for the low-energy structures at the B3LYP/LACV3P**++ level of theory for comparison to the experimentally measured IR action spectra. The calculated vibrational frequencies are scaled by 0.956, a factor found previously to provide good agreement between measured and calculated spectra in the free-OH stretch region.²² The calculated line spectra are convolved with Lorentzian peak shapes with 15 cm^{-1} fwhm for nonbonded features and 50 cm^{-1} for bonded features. Because of the very large conformational spaces of these ions, comparisons with only a limited number of structures that illustrate important bonding motifs are presented. Also, there are uncertainties associated with comparing calculated absorption spectra at zero K using the double-harmonic approximation with IR action spectra measured at 215 K.

For $\text{Cu}^{2+}(\text{H}_2\text{O})_6$, the two lowest-energy structures, **6AI** and **6AII**, each have a square planar inner shell with the two second shell water molecules each accepting two hydrogen bonds from the inner shell (Figure 8). The second-shell water molecules in

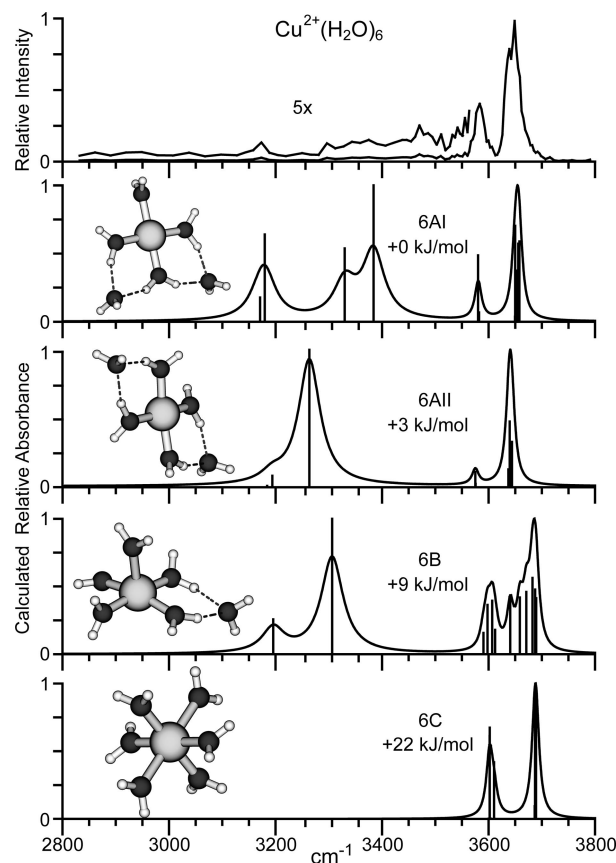


Figure 8. Infrared action spectrum of $\text{Cu}^{2+}(\text{H}_2\text{O})_6$ obtained with a copper jacket temperature of 215 K and the spectra for four low-energy conformers (**6AI**–**6C**) from B3LYP/LACV3P**++ calculations.

6AI occupy adjacent double acceptor sites whereas these molecules in structure **6AII** are opposite one another. The calculated spectra of these structures are different because of the presence of a double-donor water molecule in the former. The ν_{asym} and ν_{sym} associated with double-donor water molecules are calculated to occur in the $3300\text{--}3400 \text{ cm}^{-1}$ region whereas those of single donors are calculated to be between 3100 cm^{-1} and 3300 cm^{-1} . Structures **6B** (CN = 5) and **6C** (CN = 6) are, respectively, ~ 9 and 22 kJ/mol less stable than **6AI** at 215 K. The calculated spectra of structures **6AI** and **6AII** match the experimental spectrum well in the free-OH region, though subtle differences exist. These bands for structure **6C** are 30 cm^{-1} higher and there are no hydrogen-bonding features whereas the experimental data has significant, albeit low-intensity, photodissociation between 3100 and 3500 cm^{-1} . These results indicate that structures with a CN = 4 provide the best match to the experimental spectrum, but minor contributions from other structures cannot be ruled out.

The photodissociation intensity between 3100 and 3500 cm^{-1} relative to features in the free-OH region is much lower than predicted by the calculated absorption spectra. Even for larger clusters with significant hydrogen bonding, such as $\text{Cu}^{2+}(\text{H}_2\text{O})_8$, the relative peak intensity of the hydrogen-bonded features is

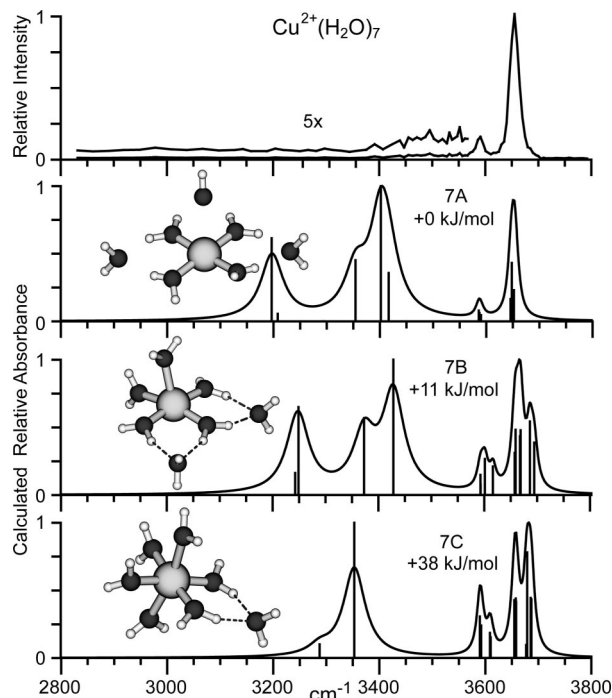


Figure 9. Infrared action spectrum of $\text{Cu}^{2+}(\text{H}_2\text{O})_7$ obtained with a copper jacket temperature of 215 K and the spectra for three low-energy conformers (7A–7C) from B3LYP/LACV3P**++ calculations.

substantially weaker than calculations predict. This discrepancy has been observed previously in the water loss IR action spectra of other clusters^{15,19,20} and has been attributed to several factors including the broadness of hydrogen-bonded bands relative to free-OH bands. OH stretching bands can broaden considerably when involved in hydrogen bonding, thereby reducing the peak intensity of these bands relative to those of the free-OH stretches.^{20,21,48,58} However, even the integrated photodissociation intensity of these bands does not account for the discrepancy indicating that other factors, such as lower photon energy, calculation uncertainties, and anharmonicity, also play a role.

For $\text{Cu}^{2+}(\text{H}_2\text{O})_7$, the free-OH region matches well with that calculated for 7A (Figure 9), the lowest-energy structure in these calculations, although the ν_{asym} and ν_{sym} bands are calculated to be $\sim 10 \text{ cm}^{-1}$ lower in frequency. The lack of distinct bands below 3550 cm^{-1} in the measured action spectrum precludes any more detailed comparison to the calculated absorption spectra.

The free-OH region of the measured spectrum of $\text{Cu}^{2+}(\text{H}_2\text{O})_8$ matches well with that calculated for 8A (Figure 10), although the calculated ν_{asym} and ν_{sym} bands are about 10 cm^{-1} lower in frequency as was the case for 7A for $\text{Cu}^{2+}(\text{H}_2\text{O})_7$. These bands for 7A are calculated to blue shift by $\sim 20 \text{ cm}^{-1}$ for 8A. This same shift is observed in the experimental action spectra of these two ions consistent with structures with CN = 4 for both cluster sizes. This shift indicates that less charge transfer occurs at $n = 8$ compared to $n = 6$ and 7 and coincides with the change in fragmentation from charge separation to water loss. In the hydrogen-bonded region of $\text{Cu}^{2+}(\text{H}_2\text{O})_8$, broad photodissociation occurs from ~ 3200 to 3600 cm^{-1} without distinct features which is somewhat surprising given the large energetic preference calculated for 8A.

Calculated spectra of some low-energy $\text{Cu}^{2+}(\text{H}_2\text{O})_{10}$ structures are shown in Figure 11. Structure 10A matches well with the experimental spectrum in the free-OH region. The experimentally observed peaks at ~ 3715 and $\sim 3630 \text{ cm}^{-1}$ match the

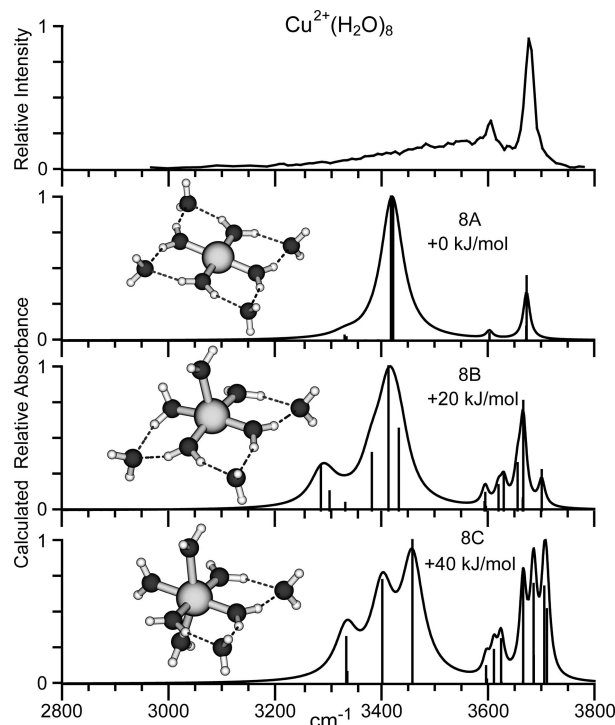


Figure 10. Infrared action spectrum of $\text{Cu}^{2+}(\text{H}_2\text{O})_8$ obtained with a copper jacket temperature of 215 K and the spectra for three low-energy conformers (8A–8C) from B3LYP/LACV3P**++ calculations.

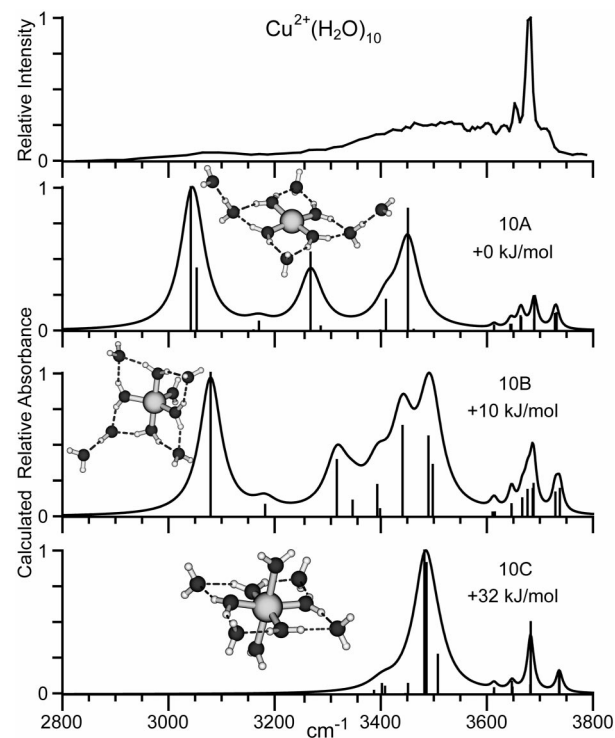


Figure 11. Infrared action spectrum of $\text{Cu}^{2+}(\text{H}_2\text{O})_{10}$ obtained with a copper jacket temperature of 215 K and the spectra for three low-energy conformers (10A–10C) from B3LYP/LACV3P**++ calculations.

free-OH ν_{asym} and ν_{sym} of single acceptors in 10A indicating the presence of water molecules in a third solvation shell. The band observed at $\sim 3690 \text{ cm}^{-1}$ corresponds to the free-OH ν_{asym} of double-acceptor water molecules and the peak at $\sim 3660 \text{ cm}^{-1}$ matches the ν_{asym} of the two AAD water molecules in 10A. These four bands become progressively more distinct for

$\text{Cu}^{2+}(\text{H}_2\text{O})_{11}$ and $\text{Cu}^{2+}(\text{H}_2\text{O})_{12}$ suggesting continued filling of the third solvation shell. The band at 3100 cm^{-1} corresponds with the hydrogen-bonded ν_{sym} of the AAD molecules in **10A** and becomes more prominent in the spectra of $\text{Cu}^{2+}(\text{H}_2\text{O})_{11}$ and $\text{Cu}^{2+}(\text{H}_2\text{O})_{12}$ further indicating the presence of additional third-shell water molecules in these larger clusters.

An exhaustive conformational search of $\text{Cu}^{2+}(\text{H}_2\text{O})_{10}$ was not performed because of the many low-energy conformations possible and the difficulty associated with identifying these conformers. Many structures similar to **10A** with CN = 4 are expected to be low in energy and should have similar calculated absorption spectra. The calculated spectrum of **10B** with CN = 5 and a single third shell water molecule is also consistent with the experimental spectrum, although the higher frequency region is not as good a match as that for **10A**. Structure **10C** with a CN = 6 is substantially higher in energy and does not have a low-frequency band attributable to third-shell water molecules. For a structure with CN = 6 to have a third-shell water molecule, a net loss of two hydrogen bonds would be necessary. Such structures are expected to be substantially higher in energy. From these calculated spectra, the experimental results for $\text{Cu}^{2+}(\text{H}_2\text{O})_{10-12}$ are found to support the formation of a third solvent shell and are consistent with a CN = 4 although contributions of structures with CN = 5 and even 6 cannot be ruled out.

Conclusions

Structures of $\text{Cu}^{2+}(\text{H}_2\text{O})_n$, $n = 6-12$, were investigated using IR action spectroscopy, blackbody infrared radiative dissociation, and density functional calculations on select cluster sizes. Results from BIRD show that cluster stability decreases with increasing size above $n = 8$, but this trend is reversed for the smaller clusters where $\text{Cu}^{2+}(\text{H}_2\text{O})_8$ is the most stable and $\text{Cu}^{2+}(\text{H}_2\text{O})_6$ is the least stable. This reversal in stability coincides with a change in the dominant fragmentation pathway from loss of a water molecule for clusters with $n \geq 9$ to a charge-separation reaction producing protonated water clusters and the corresponding singly charged hydrated metal hydroxide for $n \leq 7$. These results indicate a lower dissociation barrier for the latter reaction pathway that decreases with decreasing cluster size.

Results from density functional theory calculations for $\text{Cu}^{2+}(\text{H}_2\text{O})_n$, $n = 6-8$ and 10, indicate that the lowest-energy structures have a coordination number of 4, although structures with a CN = 5 are within about 10 kJ/mol for all clusters except $\text{Cu}^{2+}(\text{H}_2\text{O})_8$. The structure of the latter cluster is square planar with each of the four second shell water molecules accepting two hydrogen bonds from the inner-shell water molecules. These lowest-energy structures are essentially the same as those identified previously,⁴⁵ but the energy differences between these structures and those with higher coordination numbers are significantly lower with the B3LYP/LACV3P**++ level of theory.

IR action spectra provide evidence for hydrogen bonding in each of these clusters and the results for $\text{Cu}^{2+}(\text{H}_2\text{O})_n$, $n = 6-8$, are consistent with structures with CN = 4, although structures with higher CN may contribute to these spectra. New spectral features for $\text{Cu}^{2+}(\text{H}_2\text{O})_n$, $n = 10-12$, attributable to single acceptor and acceptor-acceptor-donor water molecules indicate the onset of the formation of a third solvation shell.

The axial bonding sites of Cu^{2+} are unfavorable even in the larger clusters investigated, although structures with a CN = 5 are calculated to be close in energy and such structures may contribute substantially to the measured IR action spectra for the larger clusters. With the exception of $\text{Cu}^{2+}(\text{H}_2\text{O})_8$, which

has a clear preference for a CN = 4, the relative energy differences between CN = 4 and 5 for the other gas-phase clusters are not so pronounced. The propensity to form a third solvent shell at such a small cluster size indicates that the energy differences between different CN in solution may not be large. Experiments on even larger clusters may provide additional insights of the interactions of Cu^{2+} in bulk solution.

Acknowledgment. The authors wish to thank Matthew F. Bush and James S. Prell for helpful discussions and Professor Alan G. Marshall and Dr. Gregory T. Blakney for the loan of and support for the modular data acquisition system (MIDAS). Financial support was generously provided by the National Science Foundation (Grant CHE-0718790).

References and Notes

- (1) Zeng, L.; Miller, E. W.; Pralle, A.; Isacoff, E. Y.; Chang, C. J. *J. Am. Chem. Soc.* **2006**, *128*, 10–11.
- (2) Frank, P.; Benfatto, M.; Szilagyi, R. K.; D'Angelo, P.; Della Longa, S.; Hodgson, K. O. *Inorg. Chem.* **2005**, *44*, 1922–1933.
- (3) Barnham, K. J.; Masters, C. L.; Bush, A. I. *Nat. Rev. Drug Discovery* **2004**, *3*, 205–214.
- (4) Waggoner, D. J.; Bartnikas, T. B.; Gitlin, J. D. *Neurobiol. Dis.* **1999**, *6*, 221–230.
- (5) Chaboy, J.; Muñoz-Páez, A.; Merklings, P. J.; Marcos, E. S. *J. Chem. Phys.* **2006**, *124*, 064509.
- (6) Garcia, J.; Benfatto, M.; Natoli, C. R.; Bianconi, A.; Fontaine, A.; Tolentino, H. *Chem. Phys.* **1989**, *132*, 295–307.
- (7) Beagley, B.; Eriksson, A.; Lindgren, J.; Persson, I.; Pettersson, L. G. M.; Sandström, M.; Wahlgren, U.; White, E. W. *J. Phys.: Condens. Matter* **1989**, *1*, 2395–2408.
- (8) Salmon, P. S.; Neilson, G. W. *J. Phys.: Condens. Matter* **1989**, *1*, 5291–5295.
- (9) Pasquarello, A.; Petri, I.; Salmon, P. S.; Parisel, O.; Car, R.; Tóth, E.; Powell, D. H.; Fischer, H. E.; Helm, L.; Merbach, A. E. *Science* **2001**, *291*, 856–859.
- (10) Amira, S.; Spångberg, D.; Hermansson, K. *Phys. Chem. Chem. Phys.* **2005**, *7*, 2874–2880.
- (11) Schwenk, C. F.; Rode, B. M. *J. Chem. Phys.* **2003**, *119*, 9523–9531.
- (12) Schwenk, C. F.; Rode, B. M. *ChemPhysChem* **2003**, *4*, 931–943.
- (13) Schwenk, C. F.; Rode, B. M. *J. Am. Chem. Soc.* **2004**, *126*, 12786–12787.
- (14) Kolaski, M.; Lee, H. M.; Choi, Y. C.; Kim, K. S.; Tarakeshwar, P.; Miller, D. J.; Lisy, J. M. *J. Chem. Phys.* **2007**, *126*, 074302.
- (15) Jiang, J. C.; Wang, Y. S.; Chang, H. C.; Lin, S. H.; Lee, Y. T.; Niedner-Schatteburg, G.; Chang, H. C. *J. Am. Chem. Soc.* **2000**, *122*, 1398–1410.
- (16) Headrick, J. M.; Diken, E. G.; Walters, R. S.; Hammer, N. I.; Christie, R. A.; Cui, J.; Myshakin, E. M.; Duncan, M. A.; Johnson, M. A.; Jordan, K. D. *Science* **2005**, *308*, 1765–1769.
- (17) Yeh, L. I.; Okumura, M.; Myers, J. D.; Price, J. M.; Lee, Y. T. *J. Chem. Phys.* **1989**, *91*, 7319–7330.
- (18) Miyazaki, M.; Fujii, A.; Ebata, T.; Mikami, N. *Science* **2004**, *304*, 1134–1137.
- (19) Shin, J. W.; Hammer, N. I.; Diken, E. G.; Johnson, M. A.; Walters, R. S.; Jaeger, T. D.; Duncan, M. A.; Christie, R. A.; Jordan, K. D. *Science* **2004**, *304*, 1137–1140.
- (20) Bush, M. F.; Saykally, R. J.; Williams, E. R. *ChemPhysChem* **2007**, *8*, 2245–2253.
- (21) Walters, R. S.; Pillai, E. D.; Duncan, M. A. *J. Am. Chem. Soc.* **2005**, *127*, 16599–16610.
- (22) Kamariotis, A.; Boyarkin, O. V.; Mercier, S. R.; Beck, R. D.; Bush, M. F.; Williams, E. R.; Rizzo, T. R. *J. Am. Chem. Soc.* **2006**, *128*, 905–916.
- (23) Weinheimer, C. J.; Lisy, J. M. *J. Chem. Phys.* **1996**, *105*, 2938–2941.
- (24) Rodriguez-Cruz, S. E.; Jockusch, R. A.; Williams, E. R. *J. Am. Chem. Soc.* **1998**, *120*, 5842–5843.
- (25) Rodriguez-Cruz, S. E.; Jockusch, R. A.; Williams, E. R. *J. Am. Chem. Soc.* **1999**, *121*, 8898–8906.
- (26) Rodriguez-Cruz, S. E.; Jockusch, R. A.; Williams, E. R. *J. Am. Chem. Soc.* **1999**, *121*, 1986–1987.
- (27) Wong, R. L.; Paech, K.; Williams, E. R. *Int. J. Mass Spectrom.* **2004**, *232*, 59–66.
- (28) Blades, A. T.; Jayaweera, P.; Ikononou, M. G.; Kebarle, P. *Int. J. Mass Spectrom. Ion Processes* **1990**, *102*, 251–267.

- (29) Carl, D. R.; Moision, R. M.; Armentrout, P. B. *Int. J. Mass Spectrom.* **2007**, *265*, 308–325.
- (30) Shvartsburg, A. A.; Siu, K. W. M. *J. Am. Chem. Soc.* **2001**, *123*, 10071–10075.
- (31) Stace, A. J. *Phys. Chem. Chem. Phys.* **2001**, *3*, 1935–1941.
- (32) Stace, A. J. *J. Phys. Chem. A* **2002**, *106*, 7993–8005.
- (33) Duncombe, B. J.; Duale, K.; Buchanan-Smith, A.; Stace, A. J. *J. Phys. Chem. A* **2007**, *111*, 5158–5165.
- (34) Pankewitz, T.; Lagutschenkov, A.; Niedner-Schatteburg, G.; Xanthreas, S. S.; Lee, Y. T. *J. Chem. Phys.* **2007**, *126*, 074307.
- (35) Beyer, M. K. *Mass Spectrom. Rev.* **2007**, *26*, 517–541.
- (36) Faherty, K. P.; Thompson, C. J.; Aguirre, F.; Michne, J.; Metz, R. B. *J. Phys. Chem. A* **2001**, *105*, 10054–10059.
- (37) Thompson, C. J.; Husband, J.; Aguirre, F.; Metz, R. B. *J. Phys. Chem. A* **2000**, *104*, 8155–8159.
- (38) Beyer, M. K.; Metz, R. B. *J. Phys. Chem. A* **2003**, *107*, 1760–1762.
- (39) Cox, H.; Stace, A. J. *J. Am. Chem. Soc.* **2004**, *126*, 3939–3947.
- (40) Bush, M. F.; Saykally, R. J.; Williams, E. R. *Int. J. Mass Spectrom.* **2006**, *253*, 256–262.
- (41) Cheng, Z. L.; Siu, K. W. M.; Guevremont, R.; Berman, S. S. *J. Am. Soc. Mass Spectrom.* **1992**, *3*, 281–288.
- (42) Stace, A. J.; Walker, N. R.; Firth, S. J. *Am. Chem. Soc.* **1997**, *119*, 10239–10240.
- (43) Beyer, M.; Williams, E. R.; Bondybey, V. E. *J. Am. Chem. Soc.* **1999**, *121*, 1565–1573.
- (44) Stone, J. A.; Vukomanovic, D. *Int. J. Mass Spectrom.* **1999**, *187*, 227–229.
- (45) Bércecs, A.; Nukada, T.; Margl, P.; Ziegler, T. *J. Phys. Chem. A* **1999**, *103*, 9693–9701.
- (46) Bush, M. F.; Saykally, R. J.; Williams, E. R. *J. Am. Chem. Soc.* **2007**, *129*, 2220–2221.
- (47) Fridgen, T. D.; McMahon, T. B.; MacAleese, L.; Lemaire, J.; Maitre, P. *J. Phys. Chem. A* **2004**, *108*, 9008–9010.
- (48) Iino, T.; Ohashi, K.; Inoue, K.; Judai, K.; Nishi, N.; Sekiya, H. *J. Chem. Phys.* **2007**, *126*, 194302.
- (49) Zhou, J.; Santambrogio, G.; Brümmer, M.; Moore, D. T.; Wöste, L.; Meijer, G.; Neumark, D. M.; Asmis, K. R. *J. Chem. Phys.* **2006**, *125*, 111102.
- (50) Bush, M. F.; O'Brien, J. T.; Prell, J. S.; Saykally, R. J.; Williams, E. R. *J. Am. Chem. Soc.* **2007**, *129*, 1612–1622.
- (51) Senko, M. W.; Canterbury, J. D.; Guan, S. H.; Marshall, A. G. *Rapid Commun. Mass Spectrom.* **1996**, *10*, 1839–1844.
- (52) Wong, R. L.; Williams, E. R. *J. Phys. Chem. A* **2003**, *107*, 10976–10983.
- (53) Price, W. D.; Schnier, P. D.; Jockusch, R. A.; Strittmatter, E. F.; Williams, E. R. *J. Am. Chem. Soc.* **1996**, *118*, 10640–10644.
- (54) Price, W. D.; Williams, E. R. *J. Phys. Chem. A* **1997**, *101*, 8844–8852.
- (55) Dunbar, R. C.; McMahon, T. B. *Science* **1998**, *279*, 194–197.
- (56) Herzberg, G. *Molecular Spectra and Molecular Structure II. Infrared and Raman Spectra of Polyatomic Molecules*; Van Nostrand: New York, 1945.
- (57) Shannon, R. D.; Prewitt, C. T. *Acta Crystallogr., Sect. B: Struct. Sci.* **1969**, *25*, 925–946.
- (58) Pimentel, G. C.; McClellan, A. L. *The Hydrogen Bond*; Freeman: San Francisco, 1960.

JP7115643